

1 **Immunogenicity of the Lyme Disease Antigen OspA, Particleized by Cobalt Porphyrin-**
2 **Phospholipid Liposomes**

3
4 Jasmin Federizon¹, Amber Frye^{2,3}, Wei-Chiao Huang¹, Thomas M. Hart^{2,4}, Xuedan He¹,
5 Christopher Beltran², Ashley L. Marcinkiewicz², Iain L. Mainprize⁵, Melanie K. B. Wills⁵, Yi-Pin
6 Lin^{2,3}, and Jonathan F. Lovell^{1*}

7
8
9 ¹Department of Biomedical Engineering, State University of New York at Buffalo, Buffalo, NY,
10 USA 14260

11
12 ²Division of Infectious Diseases, Wadsworth Center, New York State Department of Health,
13 Albany, New York, USA 12208

14
15 ³Department of Biomedical Sciences, State University of New York at Albany, Albany, NY, USA
16 12222

17
18 ⁴Department of Biological Sciences, State University of New York at Albany, Albany, NY, USA
19 12222

20
21 ⁵G. Magnotta Lyme Disease Research Lab, Department of Molecular and Cellular Biology,
22 University of Guelph, Guelph, ON, Canada N1G 2W1

23

24 **ABSTRACT**

25 Outer surface protein A (OspA) is a *Borrelia* lipoprotein and an established Lyme disease vaccine
26 target. Admixing non-lipidated, recombinant *B. burgdorferi* OspA with liposomes containing cobalt
27 porphyrin-phospholipid (CoPoP) resulted in rapid, particulate surface display of the
28 conformationally intact antigen. Particleization was serum-stable and led to enhanced antigen
29 uptake in murine macrophages *in vitro*. Mouse immunization using CoPoP liposomes elicited a
30 Th1-biased OspA antibody response with higher IgG production compared to other vaccine
31 adjuvants. Antibodies were reactive with intact *B. burgdorferi* spirochetes and *Borrelia* lysates,
32 and induced complement-mediated borreliacidal activity *in vitro*. One year after initial
33 immunization, mice maintained high levels of circulating borreliacidal antibodies capable of
34 blocking *B. burgdorferi* transmission from infected ticks to human blood in a feeding chamber.

35

36

37

38 **Keywords: Liposomes; Adjuvant; Particle vaccine; Lyme Disease; Borrelia; OspA**

39

40

41 **Highlights:**

42 His-tagged, recombinant *B. burgdorferi* OspA was produced and spontaneously and stably binds
43 to liposomes containing cobalt porphyrin-phospholipid (CoPoP).

44

45 Particleized OspA is effectively taken by macrophages *in vitro*.

46

47 In mice, OspA is more immunogenic when admixed with CoPoP liposomes, relative to other
48 adjuvants.

49

50 Induced antibodies recognize spirochetes and have complement-mediated borreliacidal activity.

51

52 One year after immunization, mice retain circulating OspA antibodies that block spirochete
53 transmission from infected ticks to human blood in a feeding chamber.

54

55

56

57

58 **INTRODUCTION**

59 Lyme disease, a tick-borne disease endemic in the Northern hemisphere, is a multi-organ disorder
60 caused by spirochetes belonging to the group, *B. burgdorferi* sensu lato complex.[1, 2] The main
61 etiologic agent in the United States is *B. burgdorferi* sensu stricto, whereas major pathogenic
62 genospecies in Europe also include *B. afzelii* and *B. garinii*. Without timely diagnosis and
63 treatment, this infectious disease can lead to chronic complications in the late disseminated
64 stage.[3] Due to climate change, regions of endemicity continue to expand, stressing the need for
65 effective preventive measures.[4, 5] Prophylactic immunization against Lyme disease represents
66 an attractive approach in preventing risk of contracting the disease. A leading vaccinogen is outer
67 surface protein (Osp) A, a surface lipoprotein expressed by Lyme *borreliae* while residing in the
68 tick gut. OspA expression facilitates spirochete colonization and persistence in the vector's gut
69 by binding to the tick receptor of OspA (TROSPA).[6] The mechanism of action of OspA-based
70 vaccines is based on inhibition of tick-to-human spirochete transmission, through antibody-
71 mediated borreliacidal killing, and antibody-mediated blocking of spirochete escape from the tick
72 midgut [7-9] Epitope mapping studies showed that some protective OspA antibodies recognize
73 conformational epitopes in its C-terminal domain.[10-13] Hence, it is desirable to maintain the
74 native conformation of an OspA antigen to convey protective immunity.

75 Historically, many advanced Lyme disease vaccine strategies have involved OspA.[14] Veterinary
76 vaccines available in the market incorporate bacteria-derived materials that express OspA, or
77 recombinant forms.[15-20] Valneva's VLA15, a human Lyme disease vaccine presently in clinical
78 trials, is a multivalent OspA-based vaccine.[21-23] OspA was also the vaccinogen in the LYMErix
79 vaccine which was withdrawn due in part to autoimmunity safety concerns.[24] Shorter linear
80 peptide epitopes of OspA have recently been considered for vaccine development.[25] Due to the
81 difficulty in expressing the full-length recombinant OspA in *Escherichia coli*, a truncated form of
82 OspA was constructed by eliminating the lipidation signal sequence and the adjacent cysteine

83 residue that encompass the first 17 amino acid residues. Although this deletion can improve
84 expression yield without compromising the conformational stability of the non-lipidated construct
85 [26], it consequently lowers immunogenicity.[27, 28] Co-administration of an adjuvant is thus
86 beneficial to enhance immunogenicity of non-lipidated OspA. Adjuvants are recognized as useful
87 tools for improving the efficiency of vaccines, in particular for recombinant or subunit vaccines.[29,
88 30] Liposomes serve as versatile vaccine adjuvant, and can be used to carry a wide range of
89 additional immunostimulatory molecules.[31] GSK's AS01 liposome adjuvant, which contains the
90 immunopotentiators QS-21 and monophosphoryl lipid A is an adjuvant component of the Shingrix
91 herpes zoster vaccine and RTS,S malaria vaccine [32]. Liposomes have been explored in
92 preclinical Lyme disease vaccine research [33, 34].

93 Liposome metallochelation offers a strategy to surface-functionalize nanoscale scaffolds via
94 noncovalent conjugation, using proteins with a short polyhistidine sequence (his-tag) as an anchor
95 [34]. The present study employs a self-assembling liposomal platform containing cobalt porphyrin-
96 phospholipid (CoPoP) that enables facile and serum-stable antigen functionalization with
97 aqueous incubation of his-tagged antigen with the metallochelating liposome. Inaccessibility of
98 the porphyrin moieties from the aqueous milieu has been shown to render antigen attachment
99 highly stable under physiological conditions and in the presence of large excess of competing
100 imidazole.[35] This is compared to nickel-chelated liposomes using lipid headgroup-conjugated
101 nickel nitrilotriacetic acid (Ni-NTA), which places the chelating metal exposed to the aqueous
102 environment and, for example, were shown to release a substantial amount of his-tagged in 1 hr
103 in serum at 37 °C for a his-tagged OspC Lyme disease antigen.[36] Liposomes allow for co-
104 formulation of other immunostimulatory lipid adjuvants, such as phosphorylated hexazacyl
105 disaccharide (PHAD), which can further boost immunogenicity. We previously showed that the
106 approach of using liposomes incorporating CoPoP and PHAD was effective using a malaria
107 transmission blocking antigen [37]. Lyme OspA vaccines share some similarities to malaria

108 transmission blocking vaccines in requiring antibodies that are active in the midgut of the vector
109 following a blood meal [38]. In this work, we assess antigen-functionalized liposomes formed by
110 binding his-tagged OspA to CoPoP/PHAD liposomes.

111

112 MATERIALS AND METHODS

113 *Liposome preparation and characterization*

114 CoPoP/PHAD liposomes composed of four parts 1,2-dipalmitoyl-sn-glycero-3-phosphocholine
115 (DPPC, Corden # LP-R4-057), two parts cholesterol (PhytoChol, Wilshire Technologies), one part
116 PHAD (Avanti # 699800P), and one part laboratory-made CoPoP by mass were prepared as
117 previously described [37]. In brief, liposomal components were dissolved in ethanol at 60 °C,
118 followed by slow addition of pre-heated PBS and then nitrogen-pressurized lipid extrusion at 200
119 PSI using a membrane stack of decreasing size (200, 100, and 80 nm). Extruded liposomes were
120 dialyzed in PBS at 4 °C to remove ethanol and then were characterized by dynamic light scattering
121 using NanoBrook 90Plus PALS instrument to measure liposome size and polydispersity index.
122 After determining CoPoP concentration, the liposome solution was diluted to adjust concentration
123 to 320 µg/mL CoPoP and PHAD. An analogous preparation was conducted for PoP/PHAD
124 liposomes, which lack cobalt.

125

126 *Protein expression and purification*

127 The DNA sequence encoding for non-lipidated OspA (*B. burgdorferi* B31, **Supplementary Figure**
128 **S1**) was synthesized into a pET21a plasmid by Genscript, which was transformed into BL21 (DE3)
129 competent *Escherichia coli* cells. Transformed cells were grown at 37 °C in 250 mL Luria Bertani
130 (VWR # N526) broth to an OD₆₀₀ of 0.6 - 0.8 prior to induction with isopropyl β-D-1-
131 thiogalactopyranoside (Corning # 46-102-RF). Bacterial growth continued at 22 °C overnight after
132 induction. Bacterial cells were then harvested by centrifugation, re-suspended in modified binding
133 buffer at pH 7.4, and lysed by sonication. Cell debris were pelleted by centrifugation and the

134 protein was purified from collected supernatant by immobilized metal affinity chromatography.
135 The manufacturer's recommended protocol for Ni-NTA resin (G Biosciences # 786-939) was
136 modified by including another wash buffer supplemented with 0.5 % 3-[3-
137 cholamidopropyl]dimethylammonio]-1-propanesulfonate (CHAPS, BioShop CHA003) that
138 facilitates removal of endotoxin. Pure fractions determined from SDS-PAGE (Tris-Glycine buffer
139 system) were then dialyzed to remove imidazole. Protein concentration was quantified using
140 micro-BCA assay (Thermo Fisher Scientific # 23235). Far-UV CD spectroscopic data of non-
141 lipidated OspA in 20 mM sodium phosphate pH 7.4 was acquired at room temperature on a
142 bandwidth of 1 nm, scan rate of 50 nm/min, pathlength of 0.1 cm, and accumulations of three
143 scans using Jasco J-815 CD spectrometer. Secondary structure content was calculated by
144 deconvolution of the buffer-corrected spectral data using analysis program CDSSTR and
145 reference set 7 provided by DichroWeb online server.

146

147 *Characterization of OspA binding to CoPoP/PHAD liposomes*

148 Non-lipidated, his-tagged OspA diluted to 80 μ g/mL was incubated with CoPoP/PHAD liposomes
149 at 4:1 mass ratio of CoPoP:protein, unless otherwise stated. Liposomes were then pelleted by
150 high-speed centrifugation and any unbound protein in the resulting supernatant was quantified by
151 micro-BCA assay. A non-his-tagged lysozyme (VWR # 97062-138) was used as negative control.
152 Percent binding was calculated based on the absorbance signal of the free protein. For non-
153 denaturing electrophoretic analysis, protein binding was evaluated using a histidine-MOPS buffer
154 system at near neutral pH (6.8). Due to the protein's net positive charge under native conditions,
155 polarity of the voltages applied to electrophoretic cells was reversed. Transmission electron
156 micrographs were acquired using negative staining techniques. After deposition of 10 μ L of the
157 liposome sample on carbon-coated mesh grids (Carbon type-A, 300 mesh, copper, Ted Pella #
158 01821), the grids were stained with 2% uranyl acetate. Images were then captured by JEM-2010
159 electron microscope at 200 kV using various magnifications.

160

161 *Murine vaccination and adjuvant formulations*

162 Animal experiments were conducted in accord to University at Buffalo IACUC. Eight-week-old
163 female CD-1 (ICR) mice received intramuscular injections containing 100 ng of non-lipidated
164 OspA combined with indicated adjuvants on days 0 and 21. CoPoP/PHAD and PoP/PHAD
165 liposomes were incubated with OspA at 1:4 mass ratio of protein:PHAD for 3 hr at room
166 temperature prior to injection and diluted in PBS to achieve desired antigen dose for
167 immunization. Vaccine formulation per one dose consists of 100 ng OspA, 0.4 µg CoPoP, 0.4 µg
168 PHAD, 0.8 µg cholesterol, and 1.6 µg DPPC. For commercial adjuvants, AddaVax (InvivoGen #
169 vac-adx-10) and Adju-Phos (InvivoGen, # vac-phos-250), vaccine formulations were prepared
170 according to manufacturer's instructions. For Alhydrogel 2% aluminium gel (Accurate Chemical
171 and Scientific Corporation # A1090BS), alum was mixed with the antigen to a final concentration
172 of 1.5 mg/mL. Final bleed was done on day 42 unless otherwise stated. Serum was collected after
173 centrifugation at 2,000 rcf for 15 min.

174

175 *Antibody titer and immunoglobulin isotype profiling*

176 Anti-OspA IgG titers were estimated by enzyme-linked immunosorbent assay (ELISA). A 96-well
177 plate (Thermo Scientific Nunc # 442404) was coated with 100 ng/well OspA, blocked with 2%
178 bovine serum albumin (BSA) in PBS containing 0.1% Tween-20 (PBS-T), and incubated with
179 mouse serum serially diluted in 1% BSA in PBST. After incubation with horse radish peroxidase-
180 conjugated goat anti-mouse secondary antibody IgG (Genscript # A00160), IgG1 (Invitrogen
181 A10551), or IgG2a (Invitrogen # A10685), tetramethylbenzidine (Amresco # J644) was added.
182 Endpoint titers were defined as the reciprocal serum dilution at absorbance (450 nm) cutoff of 0.5.

183

184 *OspA fluorescent labeling*

185 Prior to labeling with DY-490-NHS-Ester (Dyomics # 490-01), non-lipidated OspA was dialyzed
186 at 4 °C against sodium bicarbonate solution pH 9.3 at least twice. Stock solution of the dye was
187 added at fivefold molar excess to the protein, followed by stirring at room temperature for 2 hr.
188 Extensive dialysis against PBS was then performed to remove free dye. Post-dialysis protein
189 concentration was quantified using micro-BCA assay.

190

191 *Serum stability of liposome-bound OspA*

192 After incubation of liposomes with fluorescent-labeled OspA, human serum was added to a final
193 concentration of 20% (v/v) and then incubated at 37 °C. Aliquots were taken at different time
194 points to monitor fluorescence quenching, which directly correlates to protein binding.
195 Fluorescence measurements were acquired at excitation and emission wavelengths of 491 and
196 515 nm, respectively, on a 5 nm bandwidth using TECAN Safire multi-plate reader. Recovery of
197 fluorescence signal for CoPoP/PHAD liposomes was performed by incubating the sample in 0.1%
198 Triton X-100, 100 µg/mL proteinase K (EMD Millipore # 539480) for 30 min at 50 °C. The percent
199 fluorescence quenched was calculated by comparing to free DY490-conjugated OspA.

200

201 *Immunoprecipitation assay*

202 Following the recommended protocol for Protein G Magnetic Beads (New England Biolabs #
203 S1430S), an OspA-specific monoclonal antibody LA-2 (Absolute Antibody # Ab01070-10.0) was
204 incubated with pre-washed magnetic beads at 4 °C for at least 30 min. CoPoP/PoP/PHAD
205 liposomes with bound non-lipidated OspA were incubated with the antibody-coated magnetic
206 beads for 4 hr at room temperature. CoPoP and PoP were both included in the same liposomes
207 for fluorometric analysis. At the end of the incubation period, the beads were pelleted using a
208 magnetic separation rack after extensive washing with PBS and then re-suspended in 0.1% Triton
209 X-100, PBS to release any liposomal components. Fluorescence of the supernatant was assessed
210 at excitation and emission wavelengths of 420 and 670 nm, respectively, on a 5 nm bandwidth

211 using TECAN Safire multi-plate reader. The percent liposomes captured was calculated based
212 on a fluorescent standard curve of the liposomes, based on its PoP component. An irrelevant rat
213 monoclonal antibody we had on hand, specific for Pfs48/45, a malaria antigen, was used as a
214 negative control for immunoprecipitation.

215

216 *Nanoparticle uptake study*

217 RAW264.7 murine macrophage-like cells (ATCC # TIB-71) were cultured in a 24-well plate in
218 Dulbecco's Modified Eagle's Medium (DMEM, ThermoFisher Scientific) containing 10% fetal
219 bovine serum, 1% penicillin/streptomycin and grown to a confluence of approximately 70-80%.
220 Macrophage cells were incubated for 2 hr at 37 °C with the indicated liposome solution at OspA-
221 Dy490 final concentration of 1 µg/mL. Cytochalasin B (Acros # 228090010) was supplemented to
222 the medium at a final concentration of 10 µg/mL at least 1 hr prior to incubation with indicated
223 sample. Following incubation, macrophage cells were re-suspended in PBS and subjected to flow
224 cytometry using BD LSRIFortessa X-20 flow cytometer. FlowJo (version 10) software was used
225 for data analysis.

226 To further assess liposome uptake in macrophages, 5×10^4 RAW264.7 cells per were cultured in
227 a 96-well plate. Macrophage cells were pre-incubated with the following inhibitors: Amiloride
228 (VWR# 89152-354), Chlorpromazine (VWR# TCC2481-5G), Cytochalasin B (VWR# 200024-
229 888), Nystatin (VWR# 97062-788), and Genistein (VWR# 89148-898), at 125, 25, 5 or 1 µg/mL
230 for 1 hr. Cells were then incubated with PoP/PHAD liposomes (4 µg/mL of PoP) for 3 hr without
231 removing the inhibitors. After 3 hr of incubation, cells were washed with PBS for 3 times to remove
232 PoP/PHAD liposomes in the medium and cells were treated with 200 µl of lysis buffer (1% Triton
233 X-100 in PBS). The fluorescence signal (420 nm excitation, 670 nm emission) of PoP was
234 measured in microplate reader (TECAN Safire). Cell treated with PoP/PHAD liposomes without
235 inhibitor were used as positive control, representing 100% uptake of liposomes into macrophages.

236

237 *Western blot*
238 Bacterial cultures (*B. burgdorferi* B31, ATCC #35210; *B. afzelii* BO23, ATCC #51992, *B. garinii*
239 CIP 103362 ATCC #51383; *B. hermsii* HS1 ATCC #BAA-2821; *B. kurtenbachii* 25015 ATCC
240 #BAA-2495) grown in BSK-H media (Sigma) containing 6% rabbit serum at 33 °C, 5% CO₂ were
241 re-suspended in 1% SDS and boiled for at least 20 min, followed by centrifugation to remove
242 cellular debris. After protein quantification using DC Protein Assay (Bio-Rad), 1.5 µg of cell lysate
243 was loaded onto a 12% Tris-Glycine gel under denaturing conditions and separated proteins in
244 the acrylamide gel were transferred to a ProTran nitrocellulose membranes (GE Healthcare
245 LifeSciences) using a semi-dry Power Blotter XL (ThermoFisher Scientific). Immunoblot was
246 blocked with 1% BSA in Tris-buffered saline containing 0.1% Tween20 (TBS-T) and then
247 incubated with diluted mouse sera (1/2000) in TBS-T overnight at 4 °C. After washing, immunoblot
248 was incubated with anti-mouse secondary antibody conjugated with horse-radish peroxidase
249 (Jackson ImmunoResearch Laboratories Inc.) diluted 1/6667 in 1% BSA, TBS-T for 1.5 hr.
250 Chemiluminescence was visualized using Lumina Crescendo Western HRP Substrate (Millipore
251 Sigma).

252

253 *Indirect immunofluorescence assay*

254 For qualitative determination of specificity of IgG antibodies in mouse serum, the recommended
255 protocol for *B. burgdorferi* (strain B31) antigen substrate slides (MBL International # BB-6112)
256 was followed. A 1/500 dilution was carried out for both mouse serum antibody and DyLight488-
257 conjugated goat anti-mouse IgG secondary antibody (ImmunoReagents # GtxMu-003-
258 F488NHSX). Slides were mounted with ProLong Gold Antifade and imaged with an EVOS FL
259 microscope using a 40× objective lens.

260

261 *Splenocyte study*

262 Murine spleen collected on day 42 post-immunization was excised and passed through a sterile
263 Nylon cell strainer, followed by RBC lysis and re-suspension in Dulbecco's Phosphate-Buffered
264 Saline (Thermo Fisher Scientific). After cell counting, isolated splenocytes were diluted to 2.5 x
265 10^5 well $^{-1}$ in RPMI 1640 Medium (ThermoFisher Scientific Gibco) containing 10% fetal calf serum,
266 2 mM L-glutamine, 1 mM sodium pyruvate, 1% Eagle's medium nonessential amino acids, and
267 1% penicillin/streptomycin and then incubated with non-lipidated OspA (final concentration of 1
268 μ g/mL) for 72 hr at 37 °C. Following antigen stimulation, interferon-gamma and interleukin-4 were
269 quantified using standard ELISA based on a standard curve of the cytokine.

270

271 *Borreliacidal assay*

272 The *B. burgdorferi* strain B31-A3 used in this study is a clonal isolate of B31[39] and was cultivated
273 at 33 °C in BSKII complete medium to mid-log phase. Two-fold serial dilution of the heat-
274 inactivated mouse serum (56 °C, 30 min) was performed starting at 1/20 dilution. Then, 50 μ L of
275 the diluted serum and 10 μ L of guinea pig serum (Sigma-Aldrich # S1639) were mixed with 40 μ L
276 of BSK II complete medium containing 5×10^5 cells of *B. burgdorferi* strain B31-A3 and
277 subsequently incubated at 33 °C for 24 hr. Surviving spirochetes were quantified by direct
278 counting of motile spirochetes under dark field microscopy. Survival percentage was determined
279 from the proportion of serum-treated to untreated spirochetes. For quantitative comparison, 50%
280 borreliacidal titer, which represents the dilution rate that effectively eradicated 50% of the
281 spirochetes, was calculated using dose-response stimulation fitting in GraphPad Prism 5.04
282 (GraphPad Software, La Jolla, CA, USA).

283

284 *Feeding chamber assay*

285 Artificial feeding chambers were prepared by modifying the chamber model previously reported
286 by us and others [40-43]. The silicone rubber-saturated rayon membrane was generated as
287 described [43] and was used to mimic the hardness and elasticity of skin. Such membrane was

288 attached to one side of a 2-cm length of polycarbonate tubing (hereafter called the chamber; inner
289 diameter: 2.5 cm; outer diameter: 3.2 cm; (Amazon Inc.), as described [43]. The hair and hair
290 extract from white-tailed deer (*Odocoileus virginianus*) were generated as described [41], used
291 as feeding stimuli, and added into the chamber. Then, a 1.5-cm square of fiberglass mesh tape
292 (3-mm pore) (Lowe's Inc., Mooresville, NC), a 1.5-cm plastic tile spacer (Lowe's Inc.), a nickel
293 coin, and *I. scapularis* nymphs carrying *B. burgdorferi* strains B31-A3 (10 ticks per chamber) were
294 added onto the chamber. The chamber was then sealed using parafilm. Prior to the experiment,
295 human blood obtained from New York Blood Center (New York, NY) was defibrillated by mixing
296 with citrate-phosphate-dextrose solution (final concentration as 12.28%; Sigma). Subsequently,
297 the blood was supplemented with a cocktail of antibiotics (final concentration: 50 µg/mL rifampicin,
298 20 µg/mL phosphomycin and 2.5 µg/mL amphotericin; Sigma) to avoid microbial contamination.
299 ATP (final concentration 1µM; Sigma) and glucose (final concentration as 2 mg/mL; Sigma) were
300 also added as these reagents have been reported to enhance the efficiency of tick feeding [43].
301 The blood was added into six-well cell culture plate wells (VWR) and warmed to 37 °C, and the
302 chambers with ticks were placed on these six-well cell culture plate wells. The cell culture plate
303 wells were then placed into a 37 °C incubator with 5% of CO₂. Blood was replaced with fresh
304 blood every 24 hours. Five days post-incubation, ticks and blood were collected. DNA was then
305 extracted using Bio Basic EZ-10 Spin Column Genomic DNA Minipreps Kit for animal samples
306 following the manufacturer's instructions (Bio Basic). DNA quality and quantity were assessed for
307 each sample using a Nanodrop 1000 UV/Vis spectrophotometer (ThermoFisher) by determining
308 the concentration of DNA and the ratio of UV adsorption at 260 nm to 280 nm. The A₂₆₀:A₂₈₀ ratios
309 were between 1.75 to 1.85, which indicates the lack of RNA or proteins. Quantitative PCR (qPCR)
310 was then performed using an Applied Biosystems 7500 Real-Time PCR system (ThermoFisher)
311 to determine the presence of blood in ticks and bacterial burdens in the blood and ticks. SYBR-
312 based quantitative PCR was used to determine bacterial burdens in the ticks and blood using
313 *Borrelia* 16s ribosomal RNA primers as previously described [44].

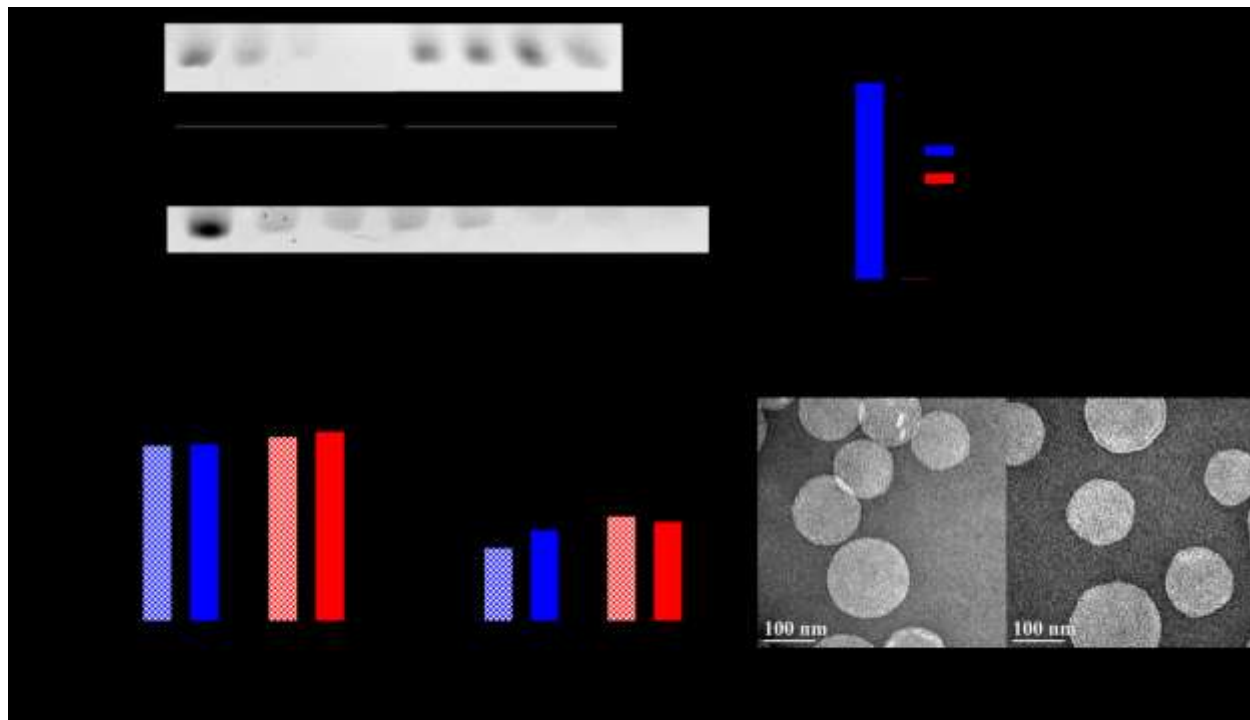
314 **RESULTS AND DISCUSSION**

315 We expressed a recombinant OspA for this study. The N-terminus lipidation signal sequence was
316 replaced with a his-tag to facilitate purification, which was carried out with Ni-NTA affinity
317 chromatography. Electrophoretic analysis indicated a homogeneous protein preparation and
318 confirmed the expected molecular weight of the purified protein, which is about 29 kDa
319 (**Supplementary Figure S2**). Structural characterization using circular dichroism spectroscopy
320 confirmed the expected foldedness of the purified protein. OspA displayed a CD spectrum with a
321 maximum at 195 nm and a minimum at 218 nm characteristic for anti-parallel β -pleated sheets
322 (**Supplementary Figure S2**). Calculated secondary structure content from the deconvolution of
323 the CD spectral data is in close agreement with the reported values in the literature.[45]

324 Spontaneous formation of the functionalized CoPoP liposomes occurs via insertion of the his-tag
325 into the hydrophobic bilayer and subsequent coordination of the imidazole moiety to the cobalt
326 center.[35, 37] Binding conditions were evaluated using native electrophoresis, which allows
327 physical separation of liposome-bound and free proteins due to the limiting pore size of the
328 acrylamide gel. An observed optimum binding mass ratio of 1:4 of OspA:CoPoP (**Figure 1A**) was
329 consistent with previous studies using the his-tagged malaria antigen, Pfs25.[37] Incubating 80
330 $\mu\text{g/mL}$ OspA with an equal volume of 320 $\mu\text{g/mL}$ CoPoP liposomes led to rapid binding of the
331 antigen (**Figure 1B**). Based upon the relative band intensities, most binding occurred between 0
332 and 15 minutes, with some additional binding occurring with longer incubation. 3 hour incubation
333 time was used for further studies. Based on a microBCA assay of the supernatant obtained from
334 high speed centrifugation, specific OspA binding is estimated to be about 80% in these conditions
335 (**Figure 1C**). Using the same method, low non-specific binding was observed for PoP/PHAD
336 liposomes, which lacks the chelating metal. A non-his-tagged protein, lysozyme, bound neither
337 CoPoP/PHAD nor PoP/PHAD liposomes. Based upon dynamic light scattering measurements,
338 post-incubation liposomal size remains close to 100 nm for both CoPoP/PHAD and PoP/PHAD

339 liposomes, with relatively monodisperse size distribution (**Figure 1D**). Transmission electron
340 micrographs revealed that CoPoP/PHAD liposomes retained their spherical morphology and size
341 close to 100 nm after antigen binding (**Figure 1E**).

342

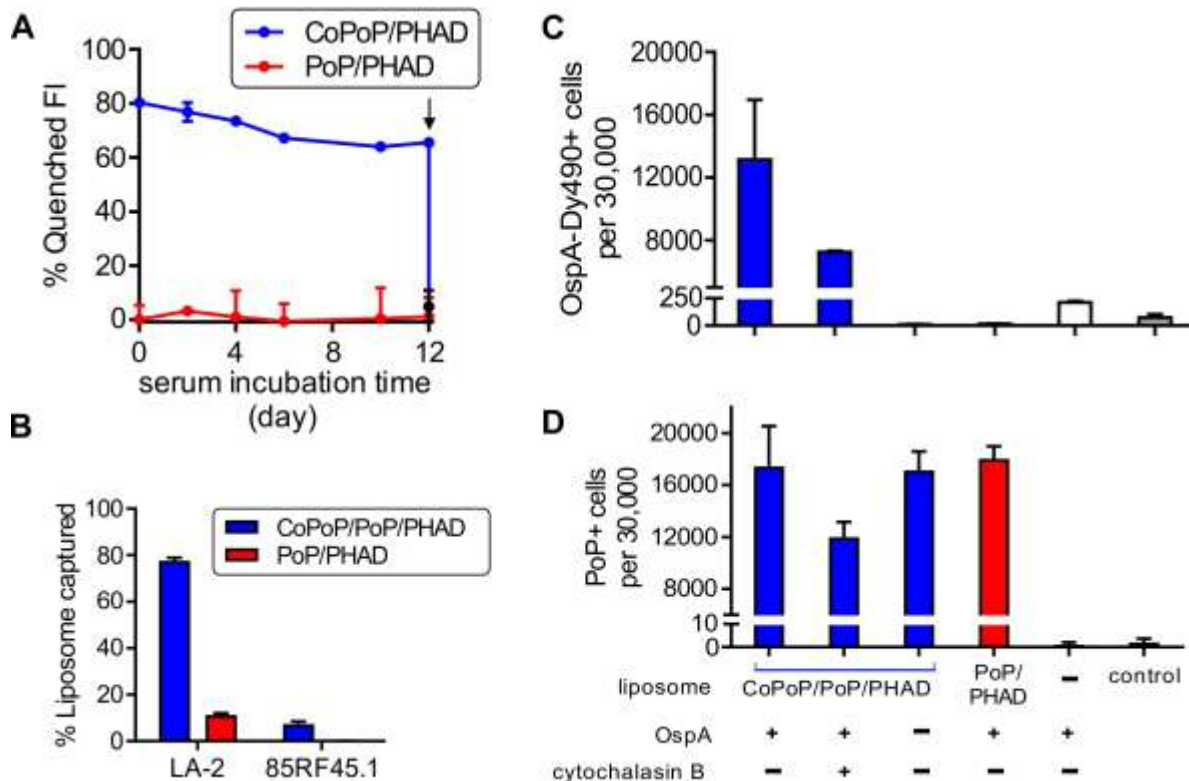


343
344 **Figure 1. Spontaneous binding of his-tagged OspA to CoPoP/PHAD liposomes. A)** Effect of
345 varying mass ratios of OspA:CoPoP/PHAD liposomes evaluated by native PAGE. The visible
346 bands that migrated in gel represent unbound protein. **B)** Kinetics of OspA binding to
347 CoPoP/PHAD liposomes incubated at 1:4 mass ratio at room temperature. **C)** Liposome binding
348 of his-tagged OspA or non-his-tagged lysozyme measured by microBCA assay of the supernatant
349 following high-speed centrifugation. **D)** Hydrodynamic diameter and polydispersity index of
350 liposomes with or without OspA incubation measured by dynamic light scattering. Error bars
351 represent standard deviations for n=3 measurements. **F)** Negative-stained electron micrographs
352 of CoPoP/PHAD liposomes with or without bound OspA.
353

354 Serum stability was assessed using fluorescently-labeled OspA (**Figure 2A**). Upon binding to
355 liposomes, the fluorescent label undergoes energy transfer to the porphyrin moieties in the bilayer
356 and the overall fluorescence becomes quenched. Incubation of OspA-bound CoPoP/PHAD
357 liposomes with human serum at 37 °C did not significantly increase the fluorescence signal after
358 12 days. This reflects that OspA remains associated to the metallochelating liposomes within the

359 duration of the study. Liposomes lacking cobalt did not bind the antigen. Serum-stable antigen
360 binding ensures integrity of the nanoparticles during transit to draining lymph nodes.

361



362

363 **Figure 2. Serum stability, epitope availability and cellular uptake of particleized OspA. A)**
364 Stability of particleized antigen association with liposomes in 20% (v/v) human serum based on
365 fluorescence quenching of dye-labeled OspA. The arrow shows restoration of OspA fluorescence
366 with detergent and protease treatment. **B)** Immunoprecipitation of OspA-bound liposomes by
367 OspA-specific monoclonal antibody LA-2. An irrelevant antibody specific for a malaria antigen
368 served as a negative control. CoPoP liposomes included additional PoP for analysis, since CoPoP
369 has weak fluorescence. Uptake of fluorescently labeled OspA (**C**) or liposomes themselves (**D**) in
370 RAW 264.7 murine macrophage cells following 2 hr incubation with indicated samples at 37 °C.
371 Cytochalasin B, a phagocytosis inhibitor, was added to medium 1 hr prior to incubation. Error bars
372 represent standard deviations for n=3 experiments.
373

374 Previous studies using analogous nanoparticle systems demonstrated variation of the
375 immunogenicity and protective efficacy with the point of attachment to the nanoparticle
376 scaffold.[46, 47] This highlights the importance of proper antigenic epitope presentation on the
377 particle surface. In this study, the his-tag was appended at the N-terminus opposite to the locality

378 of protective epitopes to ensure epitope accessibility on the liposomal surface and avoid possible
379 occlusion of the important C-terminal epitopes. This configuration putatively mimics the lipoprotein
380 integration and antigen orientation in the outer membrane of *Lyme borreliiae*. Assessment of the
381 epitope availability using a whole-liposome immunoprecipitation method confirmed surface
382 exposure and epitope intactness of the LA-2 epitope on the liposome-bound OspA (**Figure 2B**).
383 LA-2 is a protective monoclonal antibody against OspA that binds the C-terminus domain of
384 OspA.[10, 48] In this experiment, the LA-2 antibody could immunoprecipitate CoPoP liposomes
385 functionalized with OspA, based on the detection of additional PoP added to the liposomes.
386 Liposomes lacking cobalt were not immunoprecipitated. The recognition of the particleized OspA
387 by LA-2 suggests that structural integrity of the antigen is maintained after attaching to liposomes.
388 As a negative control, a rat monoclonal antibody specific for an irrelevant malaria antigen was
389 ineffective at immunoprecipitating the OspA-functionalized liposomes, although this control
390 antibody was from a different species and not isotype-matched.

391 One method for liposomes to enhance antigen delivery is based on enhanced uptake of liposomes
392 by antigen presenting cells. Nanoparticle internalization studies were assessed with flow
393 cytometry, with the gating strategy used shown in **Supporting Figure S3**. Murine macrophage
394 cells showed high antigen uptake only with the surface-functionalized liposome (**Figure 2C**).
395 Minimal uptake was observed with the free non-adjuvanted or non-associated (i.e. PoP/PHAD)
396 forms of the antigen. These results corroborate studies demonstrating enhanced antigen
397 internalization in the nanoparticulate form. In all cases, the liposomes themselves were taken
398 in macrophages, regardless of antigen attachment (**Figure 2D**). Cellular uptake of the liposome-
399 bound antigen may proceed in part via phagocytosis, which was somewhat diminished in the
400 presence of cytochalasin B, which inhibits actin polymerization.[49] Additional studies were
401 carried out to examine the uptake mechanism of PoP liposomes in the presence of selective
402 uptake inhibitors at concentrations from 1-125 μ g/mL (**Supporting Figure S4**). Besides

403 cytochalasin B, chlorpromazine, an endocytosis inhibitor that inhibits clathrin-mediated
404 endocytosis, also could effectively inhibit liposome uptake. Amiloride, genistein, and nystatin,
405 which inhibit pinocytosis or micropinocytosis through mechanisms including caveolae inhibition
406 were generally inefficient. Taken together, these data suggest that liposomes and any associated
407 antigens are taken up by macrophages (and possibly other immune cells) by endocytosis and
408 phagocytosis.

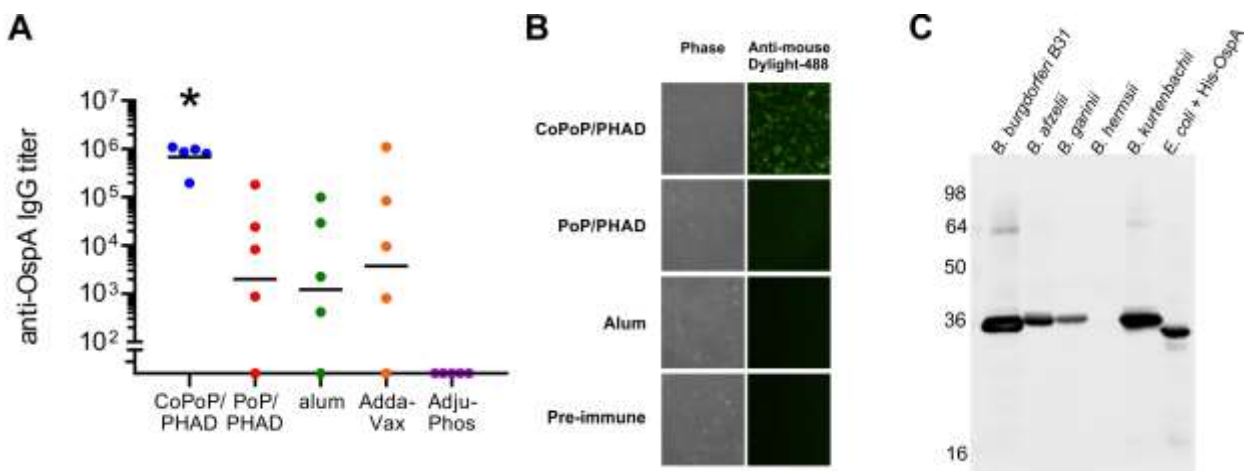
409 Next, the immunogenicity of OspA with various adjuvants was assessed in outbred CD-1 mice
410 with prime-boost intramuscular vaccination with 100 ng OspA. CoPoP/PHAD liposomes elicited
411 OspA-specific IgG antibody titer higher than other adjuvants assessed (**Figure 3A**). Otherwise
412 identical liposomes that included PHAD but lacked cobalt in the PoP macrocycle, and thus did
413 not induce OspA particle formation, exhibited lower antibody production. Although more work is
414 needed to elucidate the mechanism of the CoPoP/PHAD efficacy, enhancing antigen delivery to
415 antigen presenting cells, as implied by the *in vitro* data (**Figure 2C**), likely contributes. Other
416 adjuvants produced a lower average anti-OspA IgG titer relative to CoPoP liposomes, and higher
417 inter-subject variability was observed. Such variance in the antibody response could reflect that
418 the selected dose (100 ng) was insufficient to produce consistently high antibody response.

419 Immunofluorescence labeling of *B. burgdorferi* B31 spirochetes (**Figure 3B**) demonstrated
420 recognition by OspA-specific antibodies induced by immunization with functionalized
421 CoPoP/PHAD liposomes. Fluorescence micrographs further reveal low functional recognition of
422 the anti-OspA antibodies induced from immunization with alum and PoP/PHAD liposomes. As
423 expected, no labeling was observed for the pre-immune serum, which served as the negative
424 control.

425 Immunoblot analysis using antisera from CoPoP/PHAD immunization showed that OspA-specific
426 antibodies recognized several different strains of Lyme *borreliae* albeit to different extents (**Figure**
427 **3C**). Different band intensities reflect antigenic heterogeneity of OspA across different

428 genospecies. The relapsing fever agent *B. hermsii*, which lacks the *ospA* gene, has no visible
429 band. Minimal non-specific bands were observed for an *E. coli* lysate expressing recombinant his-
430 tagged OspA. The slightly lower molecular weight observed for the recombinant OspA band may
431 be due to the substitution of the lipidation signal sequence with a polyhistidine segment.

432

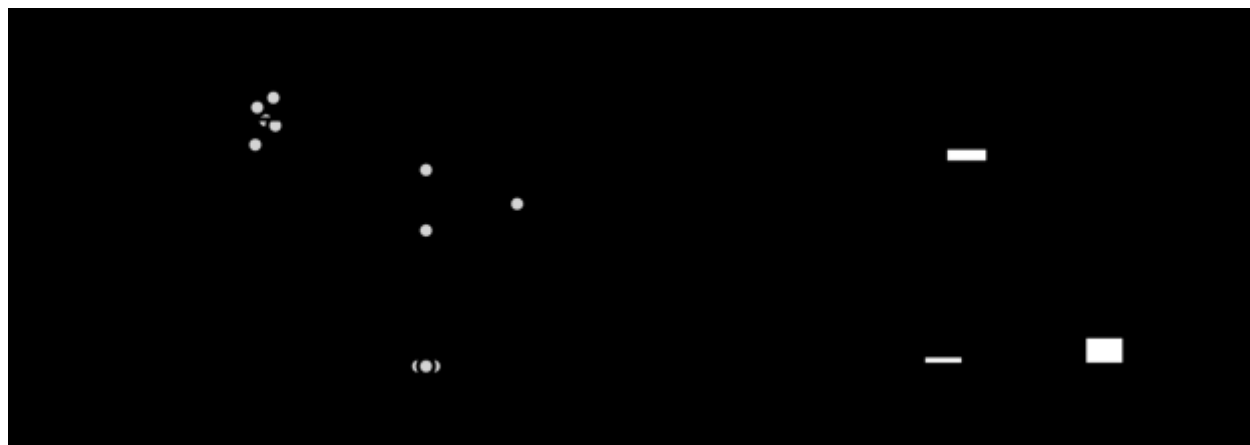


433

434 **Figure 3. Immunogenicity of OspA adjuvanted with CoPoP liposomes.** 100 ng OspA,
435 admixed with indicated adjuvants, was injected intramuscularly on day 0 and day 21 and serum
436 was collection on day 42. **A)** Anti-OspA IgG titers induced by CoPoP/PHAD liposomes compared
437 to other commercial adjuvants. Horizontal lines represent geometric mean. Asterisk shows that
438 the anti-OspA IgG titer was significantly higher in the CoPoP/PHAD adjuvant compared to all
439 others (one-way ANOVA followed by post-hoc Tukey's test; P<0.05). **B)** An indirect
440 immunofluorescence assay of *B. burgdorferi* B31 using goat anti-Mouse IgG DyLight-488
441 secondary antibody conjugate. **C)** Immunoblot assay using whole cell lysates of different *Borrelia*
442 species. CoPoP/PHAD post-immune mouse serum was used. The molecular weight size, in kDa
443 is indicated.

444

445 CoPoP/PHAD liposomes produced higher levels of OspA-specific IgG2a antibodies than IgG1
446 (**Figure 4A**). This suggests the immune response was based towards a Th1 response. Alum, on
447 the other hand, induced higher ratio levels of the IgG1 isotype. Predominance of IgG2a isotype is
448 significant as this isotype exhibits higher bactericidal activity and greater capacity to activate
449 complement than IgG1 isotype. The Th1-biased immune response observed for CoPoP/PHAD
450 liposomes correlates with the higher stimulation of interferon-gamma than interleukin-4 when
451 splenocytes from immunized mice were stimulated with OspA (**Figure 4B**).

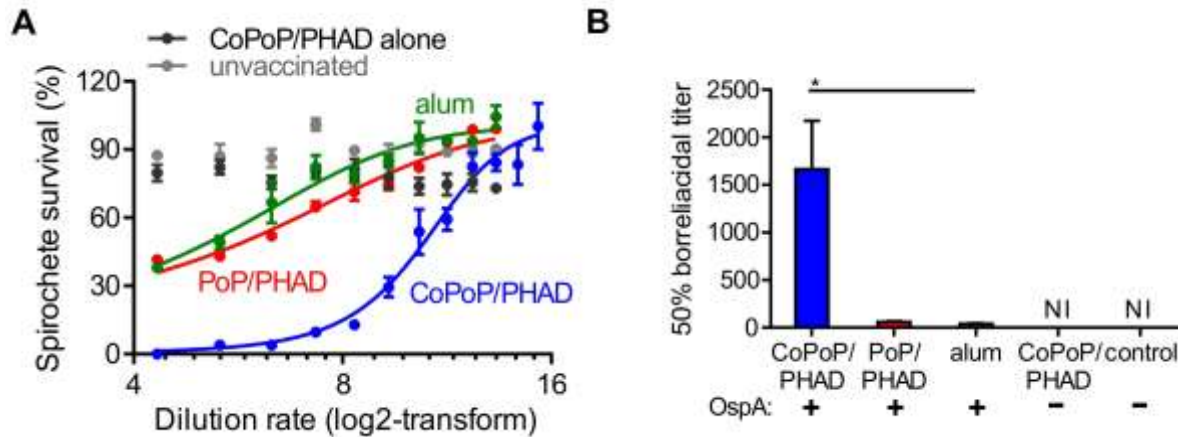


453
454 **Figure 4. Th1-biased immune response induced by OspA with CoPoP/PHAD liposomes. A)**
455 IgG isotype profiling for post-immune sera (day 42) using ELISA. Horizontal lines show geometric
456 mean. **B)** Splenocyte stimulation study to detect interferon-gamma and interleukin-4 secretion
457 after 72-hr stimulation with OspA. Splenocytes were isolated from murine spleen collected on day
458 42 post-immunization. Error bars represent standard deviations from n=3 triplicate stimulation
459 experiments.

460

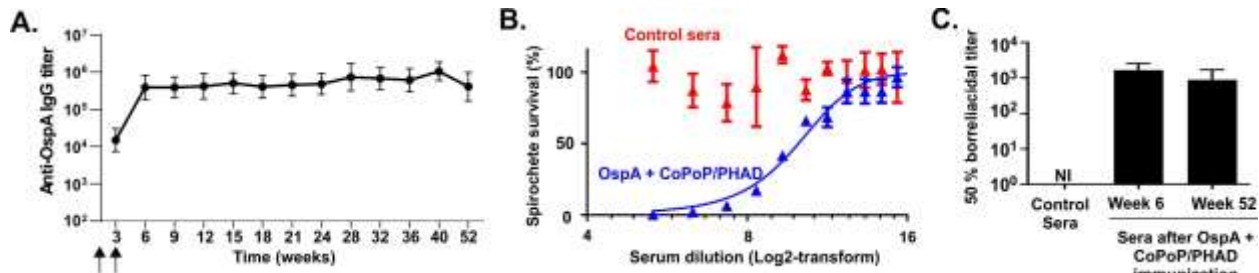
461 To demonstrate whether OspA-specific antibodies could eliminate spirochetes *in vitro*, a
462 complement-mediated bactericidal assay was performed and the borreliacidal titers were then
463 compared. Antibodies generated from CoPoP/PHAD and OspA immunization exhibited higher
464 bactericidal activity compared to OspA adjuvanted with Alum or PoP/PHAD liposomes over a
465 broad range of serum dilutions (**Figure 5A**). The calculated 50% borreliacidal titer for
466 CoPoP/PHAD liposomes was significantly higher than the other adjuvants, including Alum and
467 identical liposomes lacking cobalt (**Figure 5B**). CoPoP/PHAD liposomes themselves, without
468 addition of OspA, did not induce any complement killing.

469



470
471 **Figure 5. Borreliacidal antibodies induced by murine immunization with OspA admixed**
472 **with CoPoP/PHAD liposomes.** (A) Serum bactericidal antibody assay performed using guinea
473 pig complement incubated with varying concentrations of mouse IgG collected on day 42 after
474 priming on day 0 and boosting on day 21 with 100 ng OspA. Survival percentage was derived
475 from normalization of the number of spirochetes after overnight serum treatment to that
476 immediately after incubation. Surviving *B. burgdorferi* B31-A3 were counted using dark-field
477 microscopy. (B) Average 50% borreliacidal activity (serum dilution rate that effectively eliminated
478 50% of the bacteria) from three different mice sera. Error bars represent standard error of the
479 mean. “NI”; no inhibition. Statistical significance ($P < 0.05$, indicated by asterisk) of differences
480 between bactericidal titers is assessed by Kruskal-Wallis test with Dunn’s post-hoc analysis.

481
482
483 Protection conferred by OspA-based transmission blocking vaccines heavily relies on the levels
484 of circulating antibodies in the host blood, which enters the tick gut at the start of a blood meal.
485 Therefore, a durable antibody response is desirable for sustained vaccine efficacy. We assessed
486 long-term durability of circulating antibodies in mice following immunization with 100 ng OspA with
487 CoPoP/PHAD liposomes on day 0 and day 21. Anti-OspA IgG titers calculated at different time
488 points remained fairly similar throughout the year-long period, even up to one year after initial
489 vaccination (Figure 6A). This demonstrates a highly durable antibody response. The antibodies
490 obtained at one year post initial immunization induced similar levels complement-mediated
491 bacterial killing as those collected at 6-week post initial immunization (Figure 6B, 6C). These
492 results suggest that the CoPoP/PHAD adjuvant could potentially require less frequent booster
493 injections to retain protective antibody levels. However, it is difficult to predict the durability of the
494 immune response in other species, based on observations from mice.



495
496 **Figure 6. Longevity of anti-OspA response following immunization.** CD-1 mice were
497 immunized on day 0 and 21 with 100 ng OspA with CoPoP/PHAD liposomes **A)** Anti-OspA IgG
498 titer following immunization. Data points and error bars represent geometric mean and 95%
499 confidence interval. Arrows show days of immunization. **B)** Serum bactericidal antibody assay on
500 week 52 sera, performed using guinea pig complement incubated with varying post-immune
501 serum dilutions. **C)** Average 50% borreliacidal activity from three different mice sera. Error bars
502 represent standard error of the mean. No statistical difference of the 50% borreliacidal titer in the
503 serum collected at 6 week or one year post initial immunization. “NI”; no inhibition.

504
505
506 To verify whether the sera collected at one-year post immunization could block spirochete
507 transmission from ticks, a feeding chamber assay was used (**Figure 7A**). Human blood was mixed
508 dilute sera from CoPoP/PHAD-OspA immunized mice and infected *I. scapularis* nymphs were
509 then allowed to feed with each of these sera via our previously reported feeding chamber
510 model.[43] The bacterial burdens in ticks feeding on blood treated with sera from CoPoP/PHAD-
511 OspA-immunized mice were reduced compared to that in ticks feeding on blood incubated with
512 normal mouse sera (**Figure 7B**).

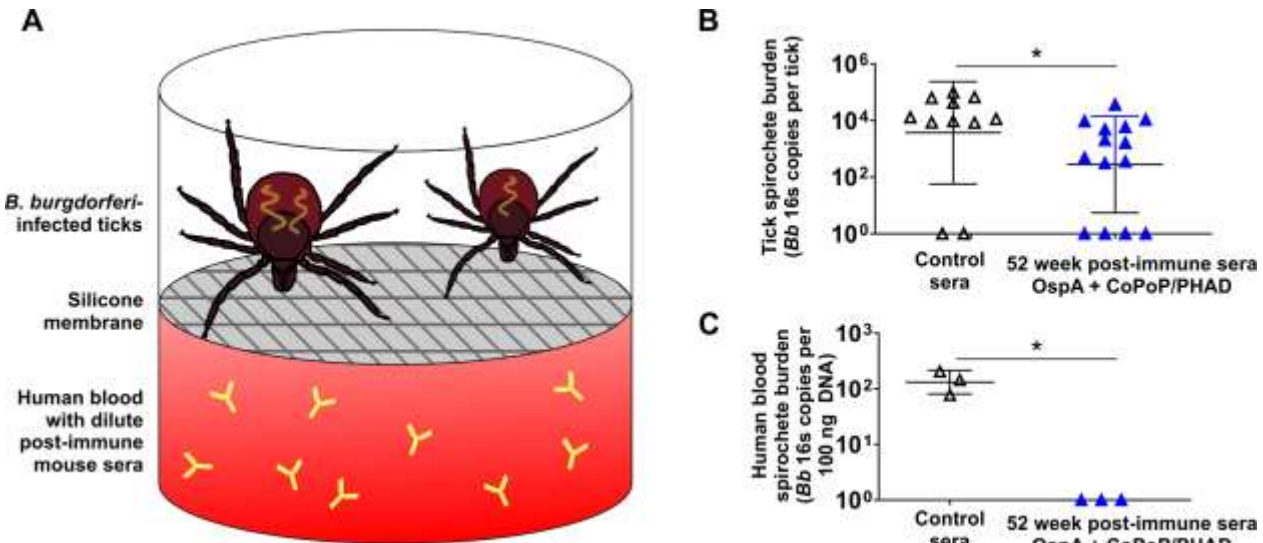
513 An OspA-based Lyme disease vaccine should inhibit the transmission of *Borrelia* from the ticks
514 to the human host, following a blood meal with the induced OspA antibodies. This could be
515 assessed in the feeding chamber (**Figure 7C**). 5 days after infected ticks were placed in the
516 feeding chamber, spirochetes could be detected in the human blood pool containing diluted
517 normal mouse sera. This shows that the bacteria migrated from the tick midgut, spread to the
518 salivary glands, and into the human blood pool. However, bacteria were undetectable in the
519 human blood mixed with post-immune sera from CoPoP/PHAD-OspA-immunized mice (one year
520 after immunization). This demonstrates that the sera from CoPoP/PHAD-OspA-immunized mice

521 was active in the tick midgut to prevent tick-borne transmission of *B. burgdorferi* for extended
522 periods following immunization with 100 ng antigen doses.

523

524

525



526
527 **Figure 7. Assessment of 52 week post-immune mouse sera using infected ticks in a human blood**
528 **feeding chamber. A)** *I. scapularis* nymphal ticks carrying *B. burgdorferi* (*Bb*) strain B31-A3 were placed in
529 feeding chambers with human blood containing diluted mouse serum (1:424 dilution) from mice immunized
530 52 weeks earlier with OspA and CoPoP/PHAD liposomes or normal mouse sera. After 5 days, nymphs
531 were pulled from the membrane and spirochete burden was determined in the ticks (**B**) or in the human
532 blood (**C**) using qPCR. Geometric mean ± geometric S.D. is shown. For ticks, *Bb* burden was determined
533 in individual ticks (11 and 14 ticks for dilute normal or post-immune mouse sera, respectively). For human
534 blood, *Bb* burden was determined on day 5 of feeding, in three feeding chambers. Asterisk indicates a
535 statistically significant difference in spirochete burden ($P < 0.05$, unpaired t-test).
536

537 This study did not assess potential toxicity of immunization with OspA and CoPoP/PHAD
538 liposomes. Previously, we reported that high doses of CoPoP itself did not induce any weight loss,
539 overt histological changes in major organs, or abnormal blood profiles.[37] Additional toxicity
540 studies are warranted with CoPoP/PHAD liposomes and OspA. Furthermore, *B. burgdorferi* OspA
541 itself has been linked with human autoimmunity based on a short epitope predicted to bind to
542 human HLA-DR4 [50]. Others have shown that this short *B. burgdorferi* OspA epitope can be
543 replaced with the analogous sequence from *B. afzelii* to address this potential problem [51]. It
544 could be useful to assess this substituted OspA antigen with CoPoP/PHAD liposomes.
545

546 **CONCLUSION**

547 CoPoP liposomes induced serum-stable binding of recombinant, his-tagged OspA while
548 preserving antigen conformation. The uptake in macrophages and immunogenicity of particleized
549 OspA was enhanced compared to other vaccine adjuvants. Vaccination with OspA admixed with
550 CoPoP/PHAD liposomes generated antibodies that recognized *B. burgdorferi* and had strong
551 borreliacidal activity. A durable, functional antibody response was observed that blocked *B.*
552 *burgdorferi* transmission from infected ticks to human blood in a feeding chamber. Taken together
553 we conclude that CoPoP liposomes warrant further investigation for use with Lyme disease
554 immunization strategies.

555

556 **ACKNOWLEDGEMENTS**

557 We thank Vladimir V. Bamm for lysate of *E. coli* expressing recombinant OspA protein. This work
558 was supported by the National Institutes of Health (R21AI122964 and DP5OD017898; JFL), the
559 National Science Foundation (1555220; JFL, IOS1755286; YL and DBI1757170; CB), the
560 Department of Defense (TB170111; YL) and the New York State Department of Health -
561 Wadsworth Center Start-Up Grant (YL).

562

563 **CONFLICTS OF INTEREST**

564 WH and JFL are named co-inventors on one or more University at Buffalo patent applications
565 describing CoPoP technology and hold equity in POP Biotechnologies, a university startup
566 company licensing the technology.

567

568

569 **REFERENCES**

570 [1] Johnson RC, Schmid GP, Hyde FW, Steigerwalt AG, Brenner DJ. *Borrelia burgdorferi* sp.
571 nov.: Etiologic Agent of Lyme Disease. *Int J Syst Evol Microbiol.* 1984;34:496-7.

572 [2] Steere AC, Grodzicki RL, Kornblatt AN, Craft JE, Barbour AG, Burgdorfer W, et al. The
573 Spirochetal Etiology of Lyme Disease. *N Engl J Med.* 1983;308:733-40.

574 [3] Steere AC, Strle F, Wormser GP, Hu LT, Branda JA, Hovius JWR, et al. Lyme borreliosis.
575 *Nat Rev Dis Primers.* 2016;2:16090.

576 [4] Dumic I, Severini E. "Ticking Bomb": The Impact of Climate Change on the Incidence of
577 Lyme Disease. *Can J Infect Dis Med Microbiol.* 2018;2018:10.

578 [5] Lindgren E, Jaenson TGT. Lyme borreliosis in Europe: influences of climate and climate
579 change, epidemiology, ecology and adaptation measures. In: Menne B, Ebi KL, editors. *Climate*
580 *Change and Adaptation Strategies for Human Health.* Geneva: Springer, Darmstadt & WHO;
581 2006. p. 157-88.

582 [6] Pal U, Li X, Wang T, Montgomery RR, Ramamoorthi N, deSilva AM, et al. TROSPA, an
583 *Ixodes scapularis* Receptor for *Borrelia burgdorferi*. *Cell.* 2004;119:457-68.

584 [7] de Silva AM, Telford SR, 3rd, Brunet LR, Barthold SW, Fikrig E. *Borrelia burgdorferi* OspA is
585 an arthropod-specific transmission-blocking Lyme disease vaccine. *J Exp Med.* 1996;183:271-5.

586 [8] Fikrig E, Telford SR, 3rd, Barthold SW, Kantor FS, Spielman A, Flavell RA. Elimination of
587 *Borrelia burgdorferi* from vector ticks feeding on OspA-immunized mice. *Proc Natl Acad Sci U S*
588 *A.* 1992;89:5418-21.

589 [9] de Silva AM, Zeidner NS, Zhang Y, Dolan MC, Piesman J, Fikrig E. Influence of outer
590 surface protein A antibody on *Borrelia burgdorferi* within feeding ticks. *Infect Immun.*
591 1999;67:30-5.

592 [10] Ding W, Huang X, Yang X, Dunn JJ, Luft BJ, Koide S, et al. Structural identification of a key
593 protective B-cell epitope in Lyme disease antigen OspA. *J Mol Biol.* 2000;302:1153-64.

594 [11] Huang X, Yang X, Luft BJ, Koide S. NMR identification of epitopes of Lyme disease antigen
595 OspA to monoclonal antibodies. *J Mol Biol.* 1998;281:61-7.

596 [12] Jiang W, Gorevic PD, Dattwyler RJ, Dunn JJ, Luft BJ. Purification of *Borrelia burgdorferi*
597 outer surface protein A (OspA) and analysis of antibody binding domains. *Clin Diagn Lab*
598 *Immunol.* 1994;1:406-12.

599 [13] Koide S, Yang X, Huang X, Dunn JJ, Luft BJ. Structure-based design of a second-
600 generation Lyme disease vaccine based on a C-terminal fragment of *Borrelia burgdorferi* OspA.
601 *J Mol Biol.* 2005;350:290-9.

602 [14] Federizon J, Lin Y-P, Lovell JF. Antigen Engineering Approaches for Lyme Disease
603 Vaccines. *Bioconj Chem.* 2019;30:1259-72.

604 [15] Conlon JA, Mather TN, Tanner P, Gallo G, Jacobson RH. Efficacy of a nonadjuvanted,
605 outer surface protein A, recombinant vaccine in dogs after challenge by ticks naturally infected
606 with *Borrelia burgdorferi*. *Vet Ther.* 2000;1:96-107.

607 [16] Levy SA. Use of a C6 ELISA test to evaluate the efficacy of a whole-cell bacterin for the
608 prevention of naturally transmitted canine *Borrelia burgdorferi* infection. *Vet Ther.* 2002;3:420-4.

609 [17] Levy SA, Millership J, Glover S, Parker D, Hogan J, Heldorfer M, et al. Confirmation of
610 Presence of *Borrelia burgdorferi* Outer Surface Protein C Antigen and Production of Antibodies
611 to *Borrelia burgdorferi* Outer Surface Protein C in Dogs Vaccinated with a Whole-cell *Borrelia*
612 *burgdorferi* Bacterin. *Intern J Appl Res Vet Med.* 2010;8:123-8.

613 [18] Chu HJ, Chavez LG, Jr., Blumer BM, Sebring RW, Wasmoen TL, Acree WM.
614 Immunogenicity and efficacy study of a commercial *Borrelia burgdorferi* bacterin. *J Am Vet Med*
615 *Assoc.* 1992;201:403-11.

616 [19] LaFleur RL, Dant JC, Wasmoen TL, Callister SM, Jobe DA, Lovrich SD, et al. Bacterin that
617 induces anti-OspA and anti-OspC borreliacidal antibodies provides a high level of protection
618 against canine Lyme disease. *Clin Vaccine Immunol.* 2009;16:253-9.

619 [20] Ball EC. Vanguard ® crLyme : Chimeric Recombinant Vaccine Technology for Broad-
620 Spectrum Protection Against Canine Lyme Disease. 2015.

621 [21] Comstedt P, Hanner M, Schüler W, Meinke A, Lundberg U. Design and Development of a
622 Novel Vaccine for Protection against Lyme Borreliosis. *PLoS One.* 2014;9:e113294.

623 [22] Comstedt P, Hanner M, Schuler W, Meinke A, Schlegl R, Lundberg U. Characterization and
624 optimization of a novel vaccine for protection against Lyme borreliosis. *Vaccine*. 2015;33:5982-
625 8.

626 [23] Comstedt P, Schüler W, Meinke A, Lundberg U. The novel Lyme borreliosis vaccine VLA15
627 shows broad protection against *Borrelia* species expressing six different OspA serotypes. *PLoS*
628 *One*. 2017;12:e0184357.

629 [24] Nigrovic LE, Thompson KM. The Lyme vaccine: a cautionary tale. *Epidemiol Infect*.
630 2007;135:1-8.

631 [25] Izac JR, Oliver LD, Earnhart CG, Marconi RT. Identification of a defined linear epitope in
632 the OspA protein of the Lyme disease spirochetes that elicits bactericidal antibody responses:
633 Implications for vaccine development. *Vaccine*. 2017;35:3178-85.

634 [26] Dunn JJ, Lade BN, Barbour AG. Outer surface protein A (OspA) from the Lyme disease
635 spirochete, *Borrelia burgdorferi*: high level expression and purification of a soluble recombinant
636 form of OspA. *Protein Expr Purif*. 1990;1:159-68.

637 [27] Erdile LF, Brandt MA, Warakomski DJ, Westrak GJ, Sadziene A, Barbour AG, et al. Role
638 of attached lipid in immunogenicity of *Borrelia burgdorferi* OspA. *Infect Immun*. 1993;61:81-90.

639 [28] Weis JJ, Ma Y, Erdile LF. Biological activities of native and recombinant *Borrelia burgdorferi*
640 outer surface protein A: dependence on lipid modification. *Infect Immun*. 1994;62:4632-6.

641 [29] Pasquale DA, Preiss S, Silva TF, Garçon N. Vaccine Adjuvants: from 1920 to 2015 and
642 Beyond. *Vaccines*. 2015;3.

643 [30] Perrie Y, Mohammed AR, Kirby DJ, McNeil SE, Bramwell VW. Vaccine adjuvant systems:
644 Enhancing the efficacy of sub-unit protein antigens. *Int J Pharm*. 2008;364:272-80.

645 [31] Alving CR. Liposomes as carriers of antigens and adjuvants. *J Immunol Methods*.
646 1991;140:1-13.

647 [32] Del Giudice G, Rappuoli R, Didierlaurent AM. Correlates of adjuvanticity: A review on
648 adjuvants in licensed vaccines. *Semin Immunol*. 2018;39:14-21.

649 [33] Beermann C, Wunderli-Allenspach H, Groscurth P, Filgueira L. Lipoproteins from *Borrelia*
650 *burgdorferi* Applied in Liposomes and Presented by Dendritic Cells Induce CD8+ T-
651 Lymphocytes in Vitro. *Cell Immunol*. 2000;201:124-31.

652 [34] Turánek J, Mašek J, Křupka M, Raška M. Functionalised Nanoliposomes for Construction
653 of Recombinant Vaccines: Lyme Disease as an Example. In: Giese M, editor. *Molecular*
654 *Vaccines: From Prophylaxis to Therapy - Volume 2*. Cham: Springer International Publishing;
655 2014. p. 561-77.

656 [35] Shao S, Geng J, Ah Yi H, Gogia S, Neelamegham S, Jacobs A, et al. Functionalization of
657 cobalt porphyrin-phospholipid bilayers with his-tagged ligands and antigens. *Nat Chem*.
658 2015;7:438-46.

659 [36] Krupka M, Masek J, Bartheldyova E, Turanek Knotigova P, Plockova J, Korvasova Z, et al.
660 Enhancement of immune response towards non-lipidized *Borrelia burgdorferi* recombinant
661 OspC antigen by binding onto the surface of metallochelating nanoliposomes with entrapped
662 lipophilic derivatives of norAbuMDP. *J Control Release*. 2012;160:374-81.

663 [37] Huang WC, Deng B, Lin C, Carter KA, Geng J, Razi A, et al. A malaria vaccine adjuvant
664 based on recombinant antigen binding to liposomes. *Nat Nanotechnol*. 2018;13:1174-81.

665 [38] Huang W-C, Sia ZR, Lovell JF. Adjuvant and Antigen Systems for Malaria Transmission-
666 Blocking Vaccines. *Advanced Biosystems*. 2018;2:1800011.

667 [39] Elias AF, Stewart PE, Grimm D, Caimano MJ, Eggers CH, Tilly K, et al. Clonal
668 polymorphism of *Borrelia burgdorferi* strain B31 MI: implications for mutagenesis in an infectious
669 strain background. *Infect Immun*. 2002;70:2139-50.

670 [40] Andrade JJ, Xu G, Rich SM. A silicone membrane for in vitro feeding of *Ixodes scapularis*
671 (Ixodida: Ixodidae). *Journal of medical entomology*. 2014;51:878-9.

672 [41] Krober T, Guerin PM. An in vitro feeding assay to test acaricides for control of hard ticks.
673 Pest management science. 2007;63:17-22.

674 [42] Ramirez-Sierra MJ, Dumonteil E. Infection Rate by *Trypanosoma cruzi* and Biased
675 Vertebrate Host Selection in the *Triatoma dimidiata* (Hemiptera: Reduviidae) Species Complex.
676 *Journal of medical entomology*. 2016;53:20-5.

677 [43] Hart T, Yang X, Pal U, Lin YP. Identification of Lyme borreliae proteins promoting
678 vertebrate host blood-specific spirochete survival in *Ixodes scapularis* nymphs using artificial
679 feeding chambers. *Ticks Tick Borne Dis*. 2018;9:1057-63.

680 [44] Marcinkiewicz AL, Dupuis AP, 2nd, Zamba-Campero M, Nowak N, Kraiczy P, Ram S, et al.
681 Blood treatment of Lyme borreliae demonstrates the mechanism of CspZ-mediated complement
682 evasion to promote systemic infection in vertebrate hosts. *Cell Microbiol*. 2019;21:e12998.

683 [45] France LL, Kieleczawa J, Dunn JJ, Hind G, Sutherland JC. Structural analysis of an outer
684 surface protein from the Lyme disease spirochete, *Borrelia burgdorferi*, using circular dichroism
685 and fluorescence spectroscopy. *Biochim Biophys Acta*. 1992;1120:59-68.

686 [46] Krupka M, Masek J, Barkocziova L, Turanek Knotigova P, Kulich P, Plockova J, et al. The
687 Position of His-Tag in Recombinant OspC and Application of Various Adjuvants Affects the
688 Intensity and Quality of Specific Antibody Response after Immunization of Experimental Mice.
689 *PLoS One*. 2016;11:e0148497.

690 [47] Walker A, Skamle C, Nassal M. SplitCore: an exceptionally versatile viral nanoparticle for
691 native whole protein display regardless of 3D structure. *Sci Rep*. 2011;1:5.

692 [48] Schaible UE, Kramer MD, Eichmann K, Modolell M, Museteanu C, Simon MM. Monoclonal
693 antibodies specific for the outer surface protein A (OspA) of *Borrelia burgdorferi* prevent Lyme
694 borreliosis in severe combined immunodeficiency (scid) mice. *Proceedings of the National
695 Academy of Sciences*. 1990;87:3768-72.

696 [49] MacLean-Fletcher S, Pollard TD. Mechanism of action of cytochalasin B on actin. *Cell*.
697 1980;20:329-41.

698 [50] Steere AC, Klitz W, Drouin EE, Falk BA, Kwok WW, Nepom GT, et al. Antibiotic-refractory
699 Lyme arthritis is associated with HLA-DR molecules that bind a Borrelia burgdorferi
700 peptide. *The Journal of Experimental Medicine*. 2006;203:961-71.

701 [51] Willett TA, Meyer AL, Brown EL, Huber BT. An effective second-generation outer surface
702 protein A-derived Lyme vaccine that eliminates a potentially autoreactive T cell epitope. *Proc
703 Natl Acad Sci U S A*. 2004;101:1303-8.

704

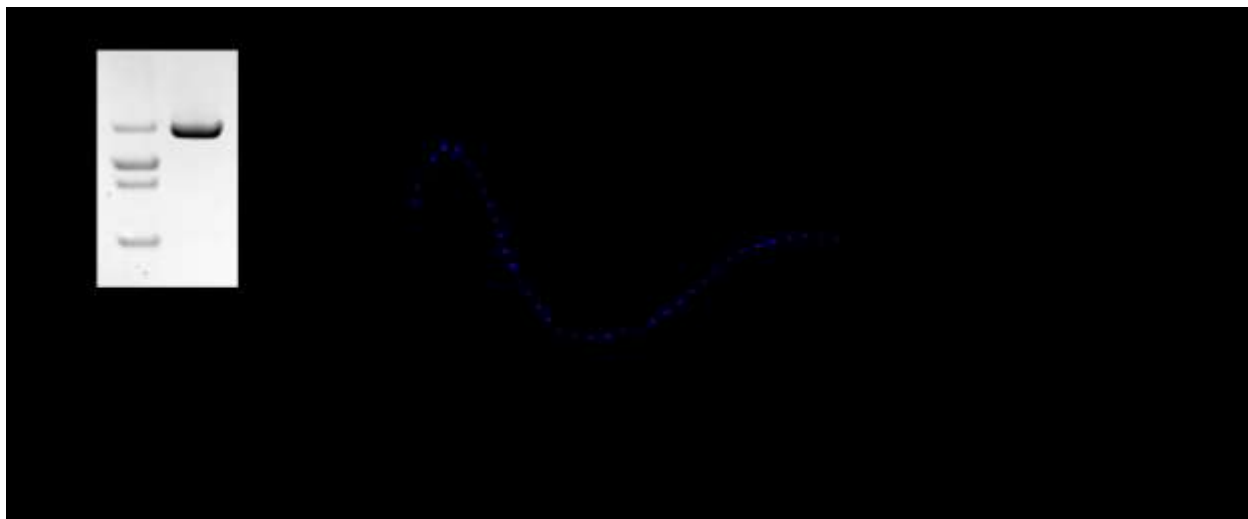
705
706
707
708
709

Supporting Information

710 MHHHHHHHHKQNVSSLDEKNSVSVDLPGEMKVLVSKENKDGKYDLIATVDKLELKGTSDKNNGSGVLEG
711 VKADKSKVKLTISDDLQQTTLLEVFKEDGKTLVSKVTSKDKSSTEKFNEKGEVSEKIIITRADGTRLEYT
712 GIKSDGSGKAKEVLKGYVLEGTTLAEKTTLVVKEGTVTLSKNISKSGEVSVELNDSSAATKKTAAWNS
713 GTSTLTITVNSKTKDLVFTKENTITVQQYDSNGTKLEGSAVEITKLDEIKNALK

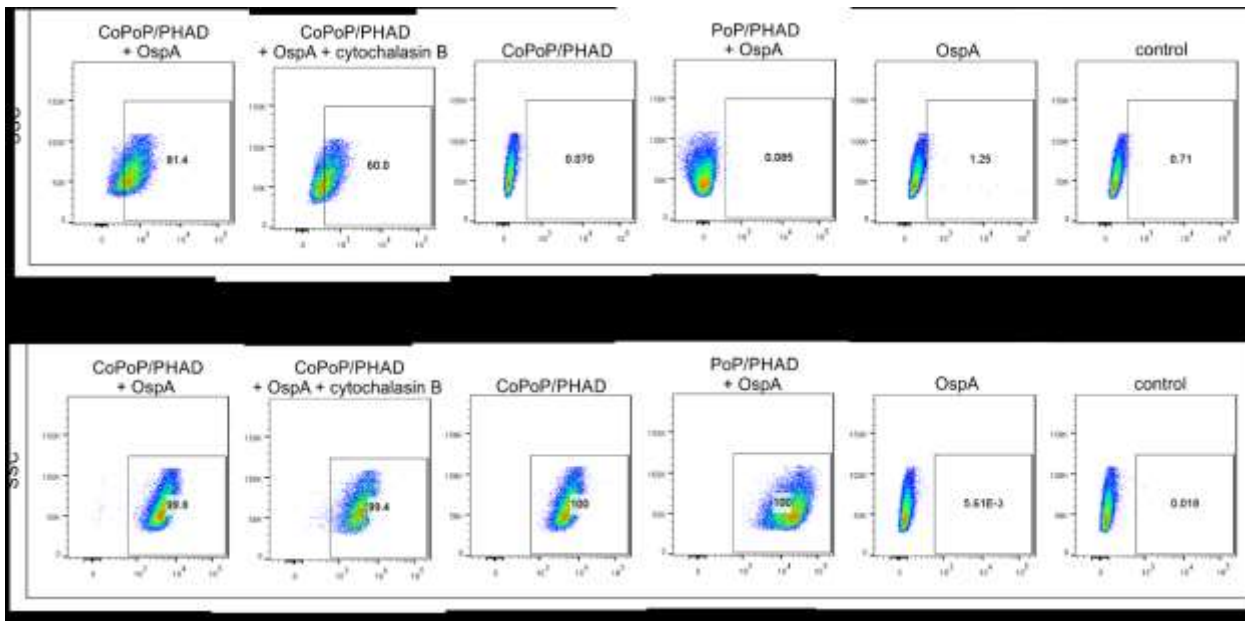
714
715 **Supplementary Figure 1.** Amino acid sequence of the recombinant non-lipidated construct of
716 *B. burgdorferi* B31. The first 17 residues (not shown) which contain the lipidation signal
717 sequence, were deleted and substituted with the his-tag.

718
719
720
721



722
723
724
725
726
727
728
729

Supplementary Figure 2. Characterization of purified recombinant non-lipidated OspA. (A) Degree of purity assessed by SDS-PAGE of 2 µg OspA (MW 29 kDa). (B) Far-UV circular dichroism spectrum of OspA in 20 mM sodium phosphate pH 7.4 solution (solid line) and calculated best fit spectrum (blue dotted line) with NRMSD of about 0.05. (C) Secondary structural content in percentage deconvoluted from buffer-corrected spectral data using CDSSTR provided by Dichroweb server.

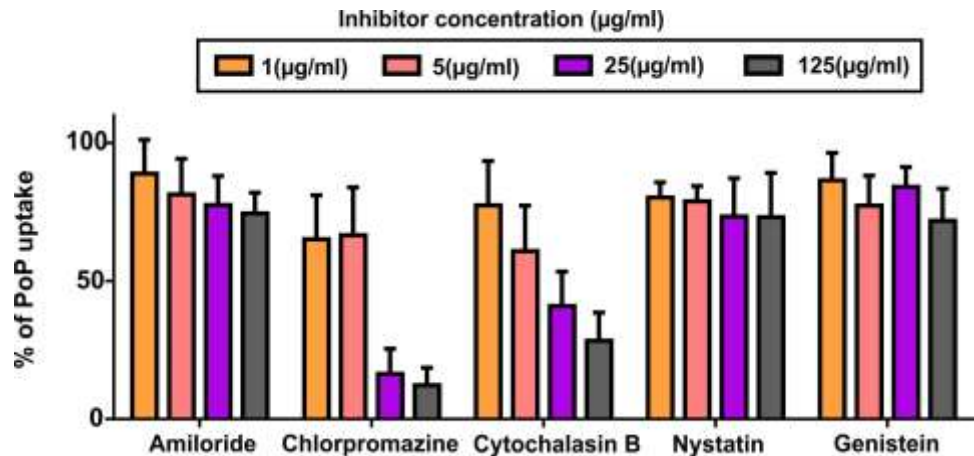


730

731 **Supplementary Figure 3.** Gating Strategy for macrophage uptake of DY-490-OspA and
 732 liposomes. Cells were first gated based on the forward and side scatter. Images are
 733 representative for three different experiments.

734

735



736

737

738

739

740

737 **Supplementary Figure 4.** Uptake of PoP liposomes in murine macrophages pretreated with
 738 indicated uptake inhibitors. PoP/PHAD liposomes were incubated with cells for 3 hr and uptake
 739 was assessed, relative to untreated cells by PoP detection in the cells lysed with 1 % Triton-X100.